A Model for Pavement Temperature Prediction

Manuel J. C. Minhoto

Bragança Polytechnic Institute –Superior School of Management and Technology

Campus de Santa Apolónia, Apartado 134, 5301-857 Bragança

Phone: +351 273 303 156; Fax: +351 273 313 051

minhoto@ipb.pt

Jorge C. Pais

University of Minho

Department of Civil Engineering, Campus Azurém, 4800-058 Guimarães, Portugal

Phone: +351 253 510 208; Fax: +351 253 510 217
jpais@civil.uminho.pt

Paulo A. A. Pereira

University of Minho

Department of Civil Engineering, Campus Azurém, 4800-058 Guimarães, Portugal

Phone: +351 253 510 200; Fax: +351 253 510 217
ppereira@civil.uminho.pt

Number of words: 7273

ABSTRACT

A finite element model has been developed to calculate the temperature of a pavement located in the Northeast of Portugal. The goal of the case study presented in this paper is the validation of this model. Input data to the model are the hourly values for solar radiation and temperature, and mean daily values of wind speed obtained from a meteorological station. The thermal response of a multilayered pavement structure is modeled using a transient thermal analysis for four months time-period (December 2003 - April 2004) and the analysis was initiated with the full depth constant initial temperature obtained from field measurements. During these four months, pavement temperature was measured at a new pavement section, located at IP4 main road, near Bragança, in the north of Portugal. At that location, seven thermocouples were installed in the AC layers, at seven different depths. These pavement data was used to validate this simulation model, by comparing model calculated data with measured pavement temperatures.
As conclusion, the 3-D finite-element analysis proved to be an interesting tool to simulate the transient behavior of asphalt concrete pavements. The suggested simulation model can predict the pavement temperature at different levels of bituminous layers with a good accuracy.

Nº of words (abstract): 201

1 - INTRODUCTION

Bituminous overlays have been the most used method in pavements rehabilitation. The service life of an overlay depends on its performance in different distress modes. In an overlay placed on a cracked pavement, the cracks will develop and propagate to the pavement surface, directly above cracks in the existing pavement under static and repetitive loading, during the first few years of service. This mode of distress is traditionally referred as "reflective cracking" and is a major concern to highway agencies throughout the world. Thus, the asphalt concrete overlay is exposed to great strains and stresses when subjected to traffic and thermal loadings. Several authors (*1*) and *(2)* suggest that different mechanisms have been identified as the origin and propagation of cracks in overlays of pavements (*1*):

1. Thermal stresses from thermal fatigue, which occurs when temperature variations induce cyclic openings and closures of cracks in the pavement, which induce stress concentrations in the overlay.
2. Thermal stresses as a result of rapid cooling down of the top layer, which induces critical tensile stresses on overlay.
3. Repetitive traffic loads induce additional distress in the overlay and increase the rate of crack propagation, whether or not these cracks originate from thermal stresses;
4. Soil movements – settlements (downwards), frost.

The literature review *(2)* also revealed that temperature variations, daily and seasonal, and associated thermal stresses, could be a cause of premature overlay cracking, affecting the predictive overlay service life of conventional and asphalt rubber mixes.

In regions that experience large daily temperatures variations or extremely low temperatures, the thermal conditions plays a major role in the reflective cracking response of a multilayered pavement structure. On one hand, binder properties (stiffness, ageing, penetration, etc…) are sensitive to temperature variations. The combination of the two most important effects: wheel loads passing above (or near) the crack and the material (overlay) above the crack being under tension due to rapidly decreasing or low temperatures, have been identified as the most likely causes of high states of stress and strain above the crack and responsible by the reflective cracking (*3*).

Daily temperature variations have an important influence in the pavement thermal state on depth below the surface of few decimeters. Depending on the level of temperature variation, stress is induced in the overlay in two different ways, which need to be distinguished: through restrained shrinkage of the overlay and through the movements of the existing slabs.

Firstly, restrained shrinkage of the overlay itself causes transverse and longitudinal tensile stresses, which are dependent of: overlay mix stiffness, overlay mix thermal coefficient of contraction, overlay mix Poisson ratio and pavement thermal gradient. These stresses have their maximum at the pavement surface, not only due the larger temperature variation, but also because of the rate dependent asphalt behavior. Due the fact that bitumen aging takes place at surface, the phenomenon described above induces the crack to initiate and propagate from the pavement surface downward. The use of softer asphalts presents as good option to delay (or arrest) reflective cracking in overlays. This thermal restrained shrinkage phenomenon occurs not only in overlays but also in new pavement structures.

Secondly, the movements of the existing slabs exert a repeated splitting at the bottom of the overlay inducing an important stress (or strain) state in the overlay. The thermal movements of cracked layer as result of thermal shrinkage are dependent of overlay mix stiffness, cracked layer mix stiffness, cracked layer mix thermal coefficient of contraction, overlay thickness, degree of friction between the overlay and distance between cracks.

Consideration should therefore be taken to the lowest expectable temperatures of the asphalt concrete. These temperatures of course differ on the weather conditions at different locations. In order to calculating thermal effects, one needs to evaluate the temperatures evolution on many depths of bituminous layers throughout typical twenty-four hours periods. The temperature distributions calculated for different times during the day allow to calculate thermal effects in the zone above the crack and can be used to investigate other affects, such as, temperature influence on layer's material properties (like stiffness) when only traffic load is considered.

Thus, the estimation of thermal response has shown that they are important. In order to consider their effects, a more precise knowledge of the temperature distribution is needed. The pavement thermal time variation state is controlled by the climatic conditions, i. e., the thermal diffusivity, as function of thermal conductivity, specific heat and density, of the materials and the depth below the surface *(2)* and *(4)*.

The temperature distribution throughout the pavement structure can be obtained through field measurements, using temperature-recording equipment (Datalogger associated with thermocouples) or estimated by using mathematical models. The option of use the field measurement is desirable because actual temperature

can be reliably measured and used in stress calculation models. However, this method is relatively slow and only provides information about temperatures in the measurement period. In other hand, a temperature model may suffer slightly due to inaccuracies but will give a temperature distribution quickly and cheaply, and can be used to predict temperature distributions under a wide range of conditions, including any unusual or extreme conditions.

The simulation model suggested in this paper is based on Finite Element Methodology, involving weather data as input. The validation of this simulation model was done by comparing output calculated data with measured pavement temperatures, obtained during December 2003 to April 2004 time period, and using measured climate data values as input, for the same time period. Also, a comparison of this simulation model with a finite difference approximation for the calculation of heat transfer down into the pavement, using general formulas for convection and radiation, and using same climate data values as input was done.

Although a one-dimensional nature of problem of the heat conduction in the vertical direction, given the infinite nature in the horizontal direction, the FEM model presented was developed in terms of three-dimensional problem in view of its future compatibility with a 3-D mechanical reflective cracking model used by the authors in other projects.

2 - BACKGROUND

The temperature distribution, at a given time, in a pavement section, is governed by heat conduction principles within pavement and by energy interaction between the pavement and its surroundings.

Conduction heat transfer

Conjugating the first law of thermodynamics, which states that thermal energy is conserved, and Fourier's law that relates the heat flux to the thermal gradients, solves the problem of heat transfer by conduction within the pavement. For an isotropic medium and for constant thermal conductivity, this principle is expressed as follow (*5*), (*6*):

$$\nabla^2 T = \frac{1}{a} \cdot \left(\frac{\partial T}{\partial t} \right)$$

where: $\nabla^2 = \left(\partial^2 / \partial x^2\right) + \left(\partial^2 / \partial y^2\right) + \left(\partial^2 / \partial z^2\right)$

$a = \dfrac{k}{r \cdot C}$ - Thermal diffusivity;

k – thermal conductivity;

ρ – density;

C – specific heat;

t - time

Interaction between the pavement and its surroundings

On a sunny day the heat transfer by energy interactions between pavement and its surroundings consists of radiation balance and exchanges by convection.

The radiation balance (or thermal radiation) involves the consideration of outgoing longwave radiation, longwave counter radiation and the shortwave radiation (or solar radiation) (*7*).

The earth surface is assumed to emit longwave radiation as a black body. Thus, the outgoing longwave radiation follows the Stefan-Boltzman law (*7*), (*5*):

$$q_e = e_e s T_s^4$$

where: q_e – outgoing radiation;

e_e – emission coefficient;

s - Stefan-Boltzman constant;

T_{sur} – pavement surface temperature.

As the atmosphere absorbs radiation and emits it as longwave radiation to the earth, this counter radiation absorbed by the pavement surface is calculated as proposed by (*7*) and (*5*):

$$q_a = e_a s T_{air}^4$$

where: q_a – absorbed counter radiation;
e_a – pavement surface absorptivity for longwave radiation and the amount of clouds;
T_{air} – air temperature.

Several authors (4) and (*8*), consider the longwave radiation intensity balance (or thermal radiation) through the follow expression:

$$q_r = h_r\left(T_{sur} - T_{air}\right)$$

where: q_r – longwave radiation intensity balance:
h_r – thermal radiation coefficient.
The expression used to obtain h_r is the following (4):

$$h_r = e\,s\left(T_{sur} + T_{air}\right)\left(T_{sur}^2 + T_{air}^2\right)$$

where: ε – emissivity of pavement surface.

Part of the high frequency (shortwave) radiation emitted by the sun is diffusely scattered in the atmosphere of the earth in all directions and the diffused radiation reached the earth is called diffused incident radiation. The radiation from the sun reaching the earth surface, without being reflected by clouds, absorbed or scattered by atmosphere, is called direct incident shortwave radiation. The total incident (direct and diffused) radiation can be estimated using the following equation *(5)*, *(6)* and (*4*):

$$q_i = h\,s_c\,f\cos q$$

where: q_i – thermal incident solar radiation;
h – loss factor accounting scattering and absorption of shortwave radiation by atmosphere;
S_c – solar constant assumed to be 1353 W/m^2;
f – factor accounting the eccentricity of earth orbit;
θ - zenith angle.

The effective incident solar radiation absorbed by pavement surface may be determined by the equation (*8*):

$$q_s = a_s \cdot q_i$$

where q_s - incident solar radiation absorbed by pavement surface;
α_s – solar radiation absorption coefficient.

In the model suggested in this paper, shortwave radiation is given as input data obtained by means of measured values.

The convection heat transfer between the pavement surface and de air immediately above it is given as (*7*) and *(4)*:

$$q_c = h_c\left(T_{sur} - T_{air}\right)$$

where: q_c – convection heat transfer;
h_c – convection heat transfer coefficient.
The convection heat transfer coefficient can be calculated as:

$$h_c = 698.24\left[\left(1.44x10^{-4}\,T_{ave}^{0.3}\,U^{0.7}\right) + \left(9.7\,x10^{-4}\left(T_{sur} - T_{air}\right)^{0.3}\right)\right]$$

where: T_{ave} – average temperature given by $T_{ave} = \left(T_{sur} - T_{air}\right)/2$;

U – wind speed.

3 -FINITE DIFFERENCE METHODOLOGY

The transient temperature response of pavements may be analysed through a numerical incremental recursive model, using a finite difference method, by applying the energy balance principle and the Fourier heat transfer equation. The thermal conductivity and thermal diffusivity of pavement are estimated with a convergence process.

The discrete form of Fourier equations within the layer can be written as (4):

$$K_i\left(\frac{T_{m-1}^p - T_m^p}{\Delta z}\right) - K_i\left(\frac{T_m^p - T_{m+1}^p}{\Delta z}\right) = r\,C\left(\frac{T_m^{p+1} - T_m^p}{\Delta t}\right)\Delta z$$

where Δt – time increment;
Δz – dept increment;

p – time superscript, is such that $\left|T^{p+1} - T^{p}\right| = \Delta t$;

m – depth superscript, is such that $\left|z_{m+1} - z_{m}\right| = \Delta z$;

K_i – thermal conductivity coefficient of layer i;

T_m^p - Temperature in the node m at time p;

ρ - density;

C – specific heat.

The discrete form of Fourier equations in the interface zone of layers can be written as (4):

$$T_m^{p+1} = \frac{2\,\Delta t}{r(\Delta z)^2}\left(K_i\,T_{m+1}^{p} + K_{i+1}\,T_{m+1}^{p}\right) + \left(1 - \frac{2K_i\,\Delta t}{r(\Delta z)^2} - \frac{2K_{i+1}\,\Delta t}{r(\Delta z)^2}\right)T_m^{p}$$

where $r = C_i\ r_i + C_{i+1}\ r_{i+1}$

Interaction between the pavement and its surroundings at surface (z=0) can be written as (4):

$$h_r\left(T_{air} - T_{sur}^{p}\right) + q_s + h_c\left(T_{sur} - T_{sur}^{p}\right) + K_i\left(\frac{T_1^{p} - T_{sur}^{p}}{\Delta z}\right) = r\,C\,\frac{\Delta z}{2}\left(\frac{T_{\sup}^{p+1} - T_{sur}^{p}}{\Delta t}\right)$$

An Excel spreadsheet was developed to solve the transient state temperature model using a finite difference method. Equations are solved incrementally at each 30-s time step in order to predict temperature at any given depth at a given time step. The model solution requires the determination of initial temperature distribution in the layers system before starting transient analysis. The initial temperature distribution adopted was obtained from field measurements.

4 - FINITE ELEMENT METHODOLOGY

This study is based on the use of the finite-element methodology in the prediction of temperature distributions in AC pavements. In the last years, this methodology has revealed a tool of great applicability in the pavements research domain. Next, the theoretical basis of this methodology and the particularization for proposed simulation model, are described.

Conduction

The first law of thermodynamics, which states that thermal energy is conserved, was used to make the resolution of pavement thermal problem through finite elements. Taking into account a differential control volume of a pavement, in that methodology the conservation of thermal energy is expressed by:

$$r\,C\,\frac{\partial T}{\partial t} + \{L\}^T\{q\} = 0$$

where: ρ - density;

C – specific heat;

T – temperature =T(x,y,z,t));

t – time;

$\{L\} = \begin{Bmatrix} \partial/\partial x \\ \partial/\partial y \\ \partial/\partial z \end{Bmatrix}$ - Vector operator;

$\{q\}$ - heat flux vector.

It should be noted that the term $\{L\}^T\{q\}$ may also be interpreted as $\nabla \cdot \{q\}$, where ∇ represents the divergence operator. Fourier's law can be used to relate the heat flux vector to the thermal gradients through the following expression:

$$\{q\} = -[D]\{L\}T$$

where: $[D]=\begin{bmatrix} K_{xx} & 0 & 0 \\ 0 & K_{yy} & 0 \\ 0 & 0 & k_{zz} \end{bmatrix}$ - conductivity matrix;

K_{xx}, K_{yy}, K_{zz} – thermal conductivity in the element x, y and z directions, respectively.

Expanding equation to its more familiar form:

$$r\,C\frac{\partial T}{\partial t}=\frac{\partial}{\partial x}\left(K_{xx}\frac{\partial T}{\partial x}\right)+\frac{\partial}{\partial x}\left(K_{yy}\frac{\partial T}{\partial y}\right)+\frac{\partial}{\partial x}\left(K_{zz}\frac{\partial T}{\partial z}\right)$$

Taking in consideration the isotropy of material ($K=K_{xx}=K_{yy}=K_{zz}$):

$$r\,C\frac{\partial T}{\partial t}=\frac{\partial}{\partial x}K\left\{\left[\left(\frac{\partial T}{\partial x}\right)+\frac{\partial}{\partial x}\left(\frac{\partial T}{\partial y}\right)+\frac{\partial}{\partial x}\left(\frac{\partial T}{\partial z}\right)\right\}\right.$$

Boundary conditions

Three types of boundary conditions were considered which cover the entire model: specified heat flow acting over the model limit surfaces; specified convection surfaces acting over superior surface of model and specified radiant energy between a superior surface and its surroundings.

Specified heat flow acting over a surface follows the general expression:

$$\{q\}^T\{h\}=-q^*$$

where: $\{h\}$ - unit outward normal vector;

q^* - specified heat flow.

Specified convection surfaces heat flows acting over a surface follows the general expression:

$$\{q\}^T\{h\}=h_f\left(T_{sur}-T_{air}\right)$$

where h_f – convection coefficient;

T_{sur} – temperature at the surface of the model;

T_{air} – bulk temperature of the adjacent fluid.

Radiant energy exchange between a surface of model and its surroundings is traduced by the follow expression, which given the heat transfer rate between the surface and a point representing the surroundings:

$$q_r=s\,e\left(T_{sur}^4-T_{air}^4\right)$$

where σ – Stefan-Boltzman coefficient;

e ? effective emissivity;

q_r – heat flux loss of surface.

3-D FEM PAVEMENT THERMAL MODEL

The 3D Finite-Element Methodology (FEM) was used to pavement thermal modeling. Traditionally, the pavement structures are idealized as a set of horizontal layers of constant thickness, homogeneous, continuous and infinite in the horizontal direction, resting on a subgrade, semi-infinite in the vertical direction. The thermal model configuration of pavement was idealized based in this principles and is presented in Figure 1. This model considers the possibility of data production to a mechanical model with the same mesh.

The used mesh was design also to study the reflective cracking due the traffic loads and is composed by a existing pavement where a crack is simulated by zero-stiffness elements and a layer on top of the existing pavement representing an overlay. This mesh was described in other works of the authors (*9*).

The finite element modeling used in the numerical thermal analysis was performed using a general Finite Elements Analysis source code, ANSYS 5.6 (*10*). This analysis is a 3D transient analysis, using a standard finite element discretization, in space based. In the design of the thermal finite-element mesh, the compatibility of mesh with other mechanical models is observed.

The following factors have been considered in the design of the finite element model:

- a finer element size is required closer to pavement surface and to wheel load point;

- a finer element size is required in the overlay above the crack;
- due to the symmetry, only half of the model needs to be modeled.

After mesh design, the number of elements was 13538. For three-dimensional thermal analysis, 3-D solid element, SOLID70, was used (Figure 2). This element, applicable to a three-dimensional transient thermal analysis, has three-dimensional thermal conduction capability, according with previous explanation. The element has eight nodes with a single degree of freedom, temperature, at each node.

The pavement material thermal properties, thermal conductivity, specific heat and density, for each pavement layer, were defined in the "material properties" of this element, when the model was developed.

For surface effect applications, like radiation exchanges convection heat transfer, the surface element SURF152 was used. The geometry, node locations, and the coordinate system for this element are shown in the Figure 3.

The element is defined by four nodes and by material properties. An extra node (away from the base element) may be used for convection and radiation effects. It was overlaid onto an area face of 3-D thermal element SOLID70, as it shows in Figure 4. The element is applicable to three-dimensional thermal analyses and allows these loads and surface effects, like heat fluxes, may exist simultaneously. The surface elements were placed on entire surface SS (Figure 1) and the extra node "M" was used to represent the air temperature.

The convection surface conductivity matrix calculation uses the convection coefficient (or film coefficient). When extra node is used, its temperature becomes the air temperature. This element allows for radiation between the surface and the extra node "M". The emissivity of the surface is used for the radiation surface conductivity matrix and the Stefan-Boltzman constant are also used for the radiation surface conductivity matrix.

The solar radiation is defined as heat flux applied on surface SS. In order to define the boundary conditions a null heat flux is applied on surfaces L1, L2, L3, L4 and SI, presented in the Figure 1.

5 - PAVEMENT TEMPERATURE PREDICTION – CASE STUDY

The goal of the case study is the validation of a FEM simulation model developed to calculate the temperatures of a pavement. A FEM numerical analysis for the distribution of temperature in a full depth asphalt pavement in a trial section located on Km 197.700 of IP4 (Bragança, Portugal) was performed for the weather conditions (air temperature, solar radiation and wind speed) from December 2003 to June 2004. The model validation was made by statistical analysis between the FEM numerical temperature results, finite differences temperature results and the field-measured temperatures.

Field data collection

During four moths (December-2003 to April-2004), pavement temperatures were measured at a newly pavement section, located at IP4 main road, near from Bragança, in the north of Portugal. At that location, seven thermocouples were installed in the AC layer, at seven different depths: at surface, 27.5 mm, 55 mm, 125mm, 165mm 220mm and 340mm. The top one was installed just at the pavement surface. The depths for the other six were chosen to give a good representation of the whole AC layers at different locations. AC temperatures were recorded every hour, every day.

With respect to short –term temperature response, it can be argued that subgrade temperature at 2.0 m depth is reasonably constant over a given months.

From a meteorological station, located near the test pavement section, it were obtained the hourly measurements of weather parameters, such as air temperature, solar radiation intensity and wind speed. These measurements were used as input data in the simulation models, to carry out temperature distribution prediction in a 340-mm full-depth pavement.

Input data to simulation

The pavement surface thermal emissivity for estimating the longwave radiation intensity balance was chosen as 0.9 and the solar absorption coefficient was chosen as 0.95. Table I presents the values for pavement material thermal properties adopted in this study. The parameters have been adapted to give a good correspondence between measured and calculated pavement temperatures. This adoption was made without an optimization process. The adopted value follows typical values for those parameters, on basis of bibliography (*3*), *(4)*, (*2*) and (*7*).

According the results from simulation made by (*7*), the influence of the thermal conductivity of the pavement is marginal for the pavement temperatures closed to the surface. Thus, no further effort was made, in this paper, to study the influence of thermal conductivity variation.

Analysis Procedure

The thermal response of FEM simulation model, representing a multilayered pavement structure, was modeled using a transient thermal analysis for a four months time-period (from December 2003 to April 2004). It is assumed that the pavement hourly temperature profile depends entirely on hourly air temperature value, hourly solar radiation value and wind speed daily mean value.

The analysis procedure involves a multiple 3-D finite-element runs and was initiated with the full depth at constant initial temperature, obtained from field measurements, and was carried out for a period between December 2003 and June 2004, with a periodicity of one hour.

For finite differences based thermal response analysis same considerations must be done.

Results

As a measure of the error, the absolute difference between measured and calculated pavement temperatures has been calculated for every hour. Then, the average difference has been determined for each month and for total time-period, referred as average errors. Table II presents the result of this procedure and in Table III the standard deviation of errors is presented. The Figures 5 until 12, shows temperatures distributions in the months January, 2004, March and April, 2004, located at surface, 55mm-depth and 165mm-depth, where good correlation were obtained between the in-situ measurements and calculated temperature.

Conclusions

The 3-D finite-element analysis proved to be an interesting tool for simulates the transient behavior of asphalt concrete pavement temperature. The suggested simulation model can, according to comparisons with field measurements, model the pavement temperature at different levels of bituminous layers with a good accuracy. To obtain this, a series of climatic data is needed as input to the model. The use of the results for other FEM mechanical models constitutes an advantage of the proposed model.

When comparing measured and calculated temperature data for every hour for a time period of four months, an average error less than 2.1 ºC was obtained in depths close to surface. At depth 340 mm the average error may reach 4 ºC at April. In cold months the average error is less than in hot months. Thus, in the cold months, the developed model presents better performance than in hot months.

The average error produced by FEM simulation model is closed to the average error produced by finite difference methodology. The small observed variations of errors between these models can be due the fact of the consideration of an average wind speed in FEM model.

The three-dimensional FEM model presents equally good results than one-dimensional nature models.

6 - ACKNOWLEDGMENT

The authors wish to acknowledge the work and technical support from Bragança Delegation of Portuguese Road Administration (Instituto de Estradas de Portugal – Direcção de Bragança).

7 - REFERENCES

1. Sousa, Jorge B., Pais, Jorge C., Saim, Rachid, Way, George &, Stubstad, Richard N.. Development of a Mechanistic-Empirical Based Overlay Design Method for Reflective Cracking In *Transportation Research Record: Journal of the Transportation Research Record, Nº 1809 - paper number 02-2846,* TRB, National Research Council. Washington, D.C. 2002, pp 209-217.
2. de Bondt Arian. Effect of Reinforcement Properties. Proceedings PRO11. 4th International RILEM Conference on Reflective Cracking in Pavements – Research in Practice. Edited by A. O. Abd El Halim, D. 5. A. Taylor and El H. H. Mohamed. RILEM. Ottawa, Ontario, Canada. March, 2000, pp 13-22.

3. A. Shalaby, Abd el Halim A.O and O.J. Svec. Low-temperature stresses and fracture analysis of asphalt overlays. Proceedings. In *Transportation Research Record: Journal of the Transportation Research Record, Nº 1539*, TRB, National Research Council. Washington, D.C.. 1990. pp 132-139.
4. Donath M., Mrawira and Joseph Luca. Thermal Properties and Transient Temperature Response of Full-Depth Asphalt Pavements. In *Transportation Research Record: Journal of the Transportation Research Record, Nº 1809 - paper number 02-4100*, TRB, National Research Council. Washington, D.C. 2002, pp 160-169.
5. Dewit D. P. and F. P. Incopera . Fundamentals of Heat and Mass transfer. Edited by John Wiley and Sons. Toronto, Canada. 1996.
6. Ozisik M. N.. Heat Transfer: A Basic Approach. Edited by McGraw-Hill. New York, USA. 1985.
7. Hermansson A.. A Mathematical Model for Calculating Pavement Temperatures, Comparisons between Calculated and Measured Temperatures. Transportation Research Record: Journal of the Transportation Research Record, Nº 1764 – paper number 01-3543. National Research Council. Washington, D.C.. 2001.
8. Picado-Santos L.. Consideração da Temperatura no Dimensionamento de Pavimentos Rodoviários Flexíveis. Ph. D. Tesis. University of Coimbra. Lisbon. 1994.
9. Minhoto, Manuel J.C., Pais, Jorge C., Pereira, Paulo A.A. & Picado-Santos, Luís G., "Low-Temperature Influence in the Predicted of Pavement Overlay", Asphalt Rubber 2003 Conference, Brasilia, Brasil, 2003, p. 167-180.
10. ANSYS 5.6 – computer program. ANSYS Theory Reference – Realise 5.6. Edited by Peter Kohnke. ANSYS Inc.Canonsburg. 1999.

List of Tables and Figures

List of Tables

List of Figures

Tables

Table I – Layers Thermal Properties

	Thickness (m)	K (W/ºC.m)	C (W.s/kg.ºC)	density (Kg/m^3)
Overlay – wearing course	0.055	1.5	850	2550
Overlay – basecourse	0.070	1.5	860	2350
Cracked layer	0.215	1.5	850	2550
Sub-base	0.300	1.5	805	2370
subgrade	-	1.79	1100	2200

Table II – Average errors results

		Average errors													
	Depth >	0 mm		27.5 mm		55 mm		125 mm		165 mm		220 mm		340 mm	
Month	Method >	Fin. Dif.	FEM	Fin. Dif.	FEM	Fin. Dif.	FEM	Fin. Dif.	FEM	Fin. Dif.	FEM	Fin. Dif.	FEM	Fin. Dif.	FEM
December		1.7305	2.1892	1.5251	1.9867	1.3084	1.7164	1.1059	1.3043	1.184	1.0978	1.4373	0.9521	2.6714	2.1224
January		1.6697	1.6985	1.4632	1.5323	1.3639	1.3754	1.2304	1.1993	0.9665	0.9327	0.7856	0.7229	1.7828	1.9414
Febrary		1.3608	1.3675	1.1767	1.2076	1.062	1.0318	0.7143	0.7055	1.0661	0.9145	0.7122	0.6951	2.613	2.4323
March		1.3604	1.3878	1.1726	1.2091	1.2069	1.179	1.5942	1.3959	1.8198	1.4972	1.0481	0.8016	2.8134	2.647
April		2.0394	2.0085	1.9417	2.0141	1.7611	1.6663	2.0518	1.8459	2.2845	1.9264	1.4738	1.2073	4.2292	4.0886
December-April		1.6441	1.6825	1.4745	1.5572	1.3719	1.3665	1.4168	1.3238	1.5311	1.3234	1.0538	0.8773	2.8677	2.7632

Table III – Standard Deviation of errors

		Standard deviation of errors													
	Depth >	0 mm		27.5 mm		55 mm		125 mm		165 mm		220 mm		340 mm	
Month	Method >	Fin. Dif.	FEM	Fin. Dif.	FEM	Fin. Dif.	FEM	Fin. Dif.	FEM	Fin. Dif.	FEM	Fin. Dif.	FEM	Fin. Dif.	FEM
December		1.1553	1.5899	0.9263	1.3457	0.9026	1.0678	0.9149	0.7346	0.9236	0.6562	0.6885	0.64	1.6151	1.0578
January		1.3382	1.3795	1.202	1.2571	1.0186	1.0798	0.8126	0.8333	0.6854	0.7742	0.5209	0.6305	1.3446	1.1094
Febrary		1.0773	1.0843	0.82	0.8782	0.7761	0.7716	0.5463	0.5452	0.7522	0.6973	0.5073	0.4846	1.7641	1.4332
March		1.2977	1.3246	0.9796	1.0594	1.0747	1.0601	1.1578	1.1019	1.3582	1.1674	0.9383	0.8001	2.1728	2.0396
April		1.6421	1.6259	1.312	1.3569	1.2859	1.2365	1.3	1.2326	1.7471	1.4497	0.8732	0.7271	2.8718	2.6089
December-April		1.3871	1.4314	1.1469	1.2349	1.0899	1.0955	1.1144	1.0416	1.3367	1.1404	0.8002	0.7045	2.2874	2.0395

Figures

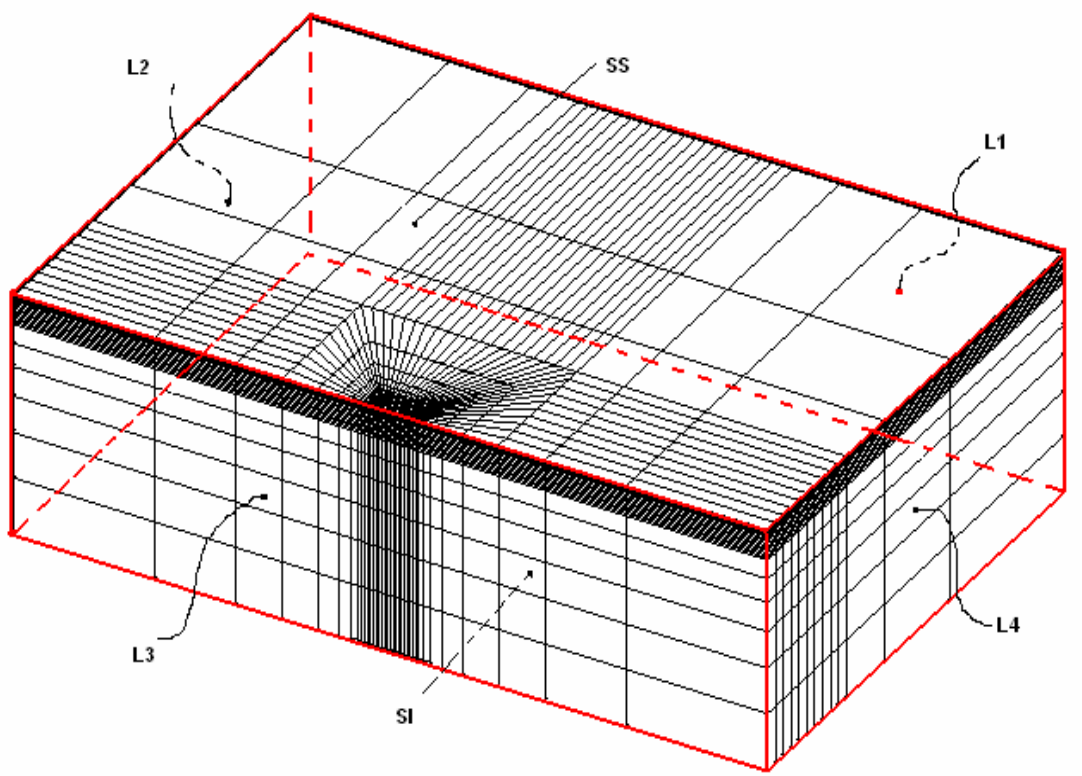

Figure 1 – FEM mesh Thermal model

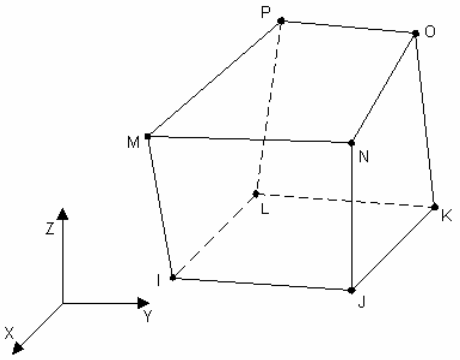

Figure 2 – 3-D Thermal Solid element (SOLID70)

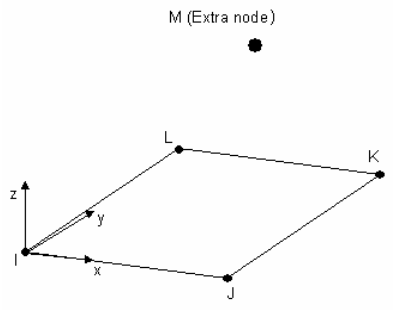

Figure 3 – Surface Thermal element (SURF152)

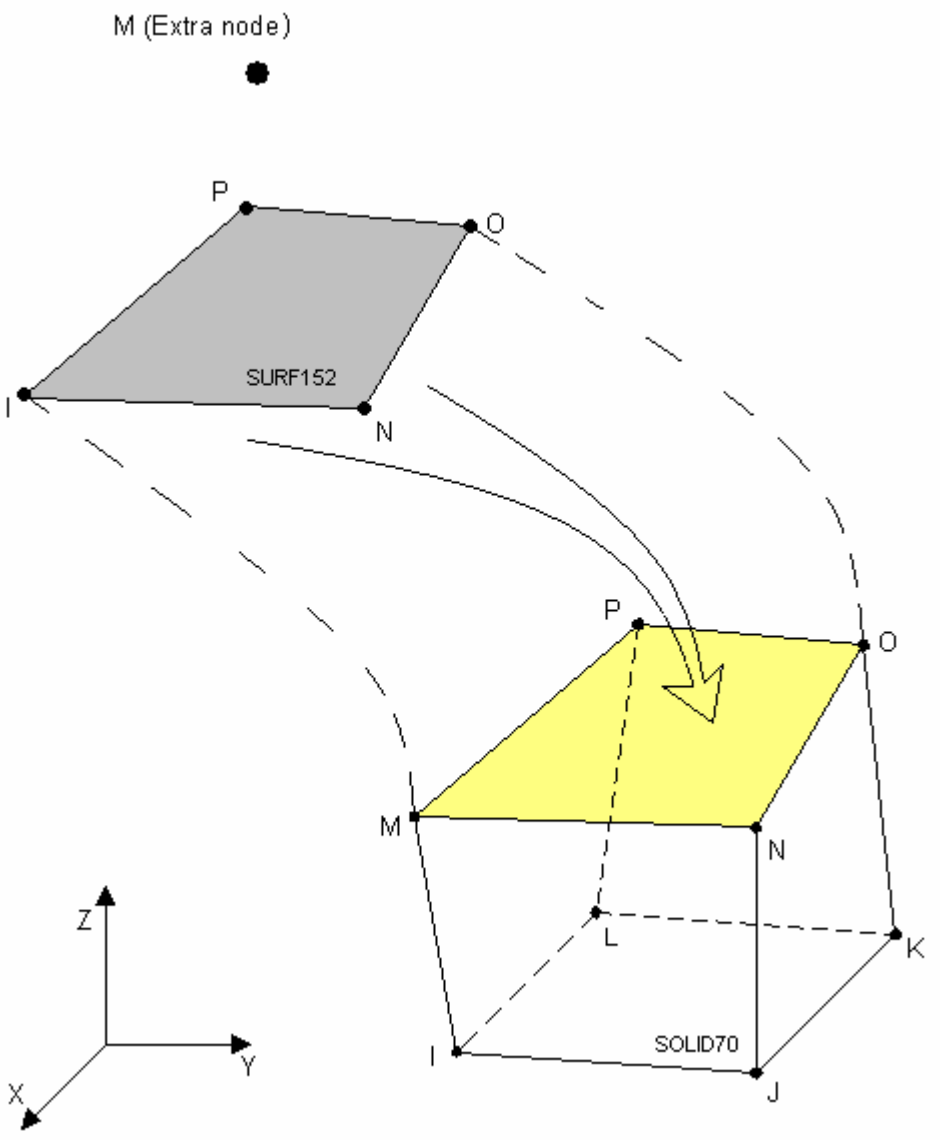

Figure 4- SURF152 and SOLID70 coupling

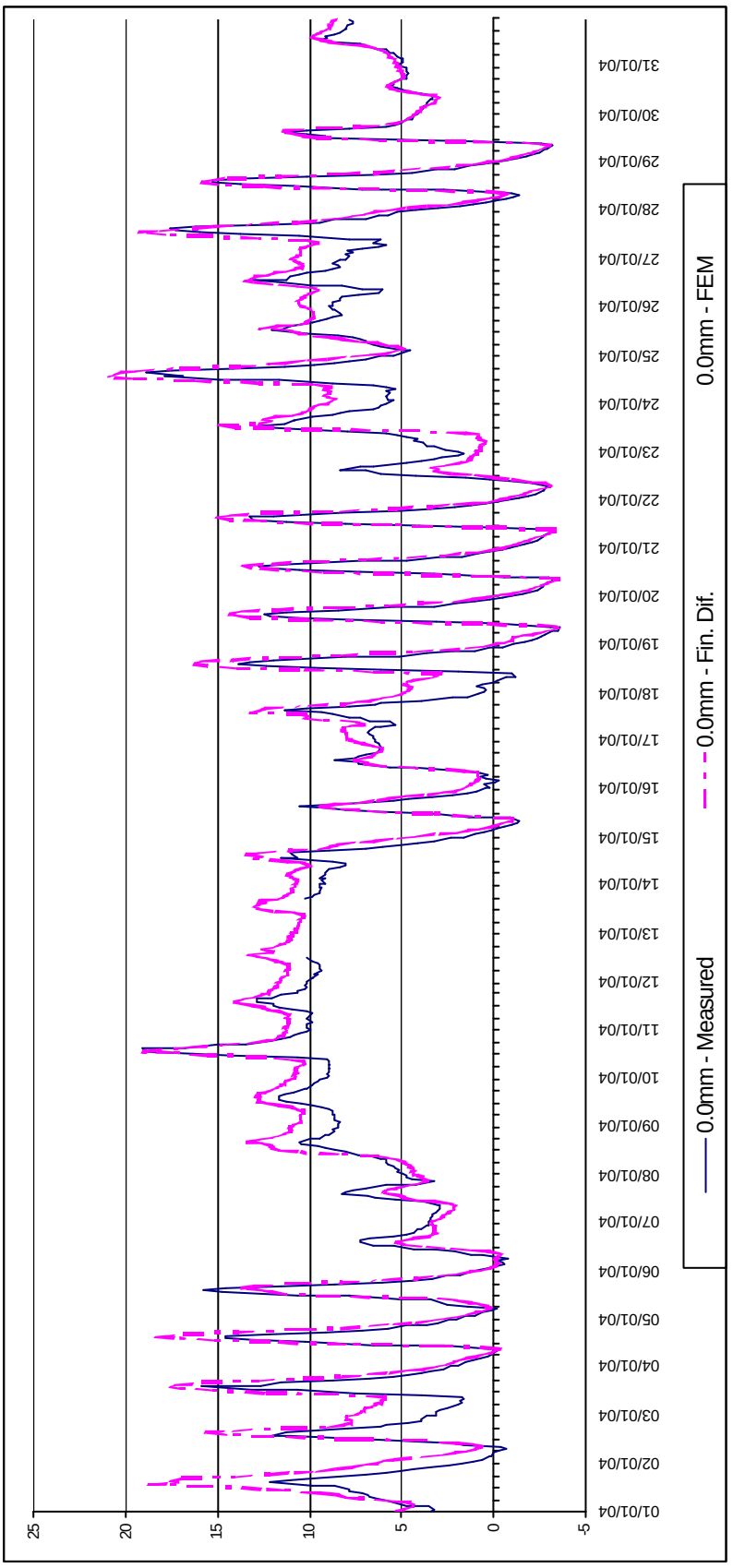

Figure 5 – January 0.0 mm-depth temperature distribution

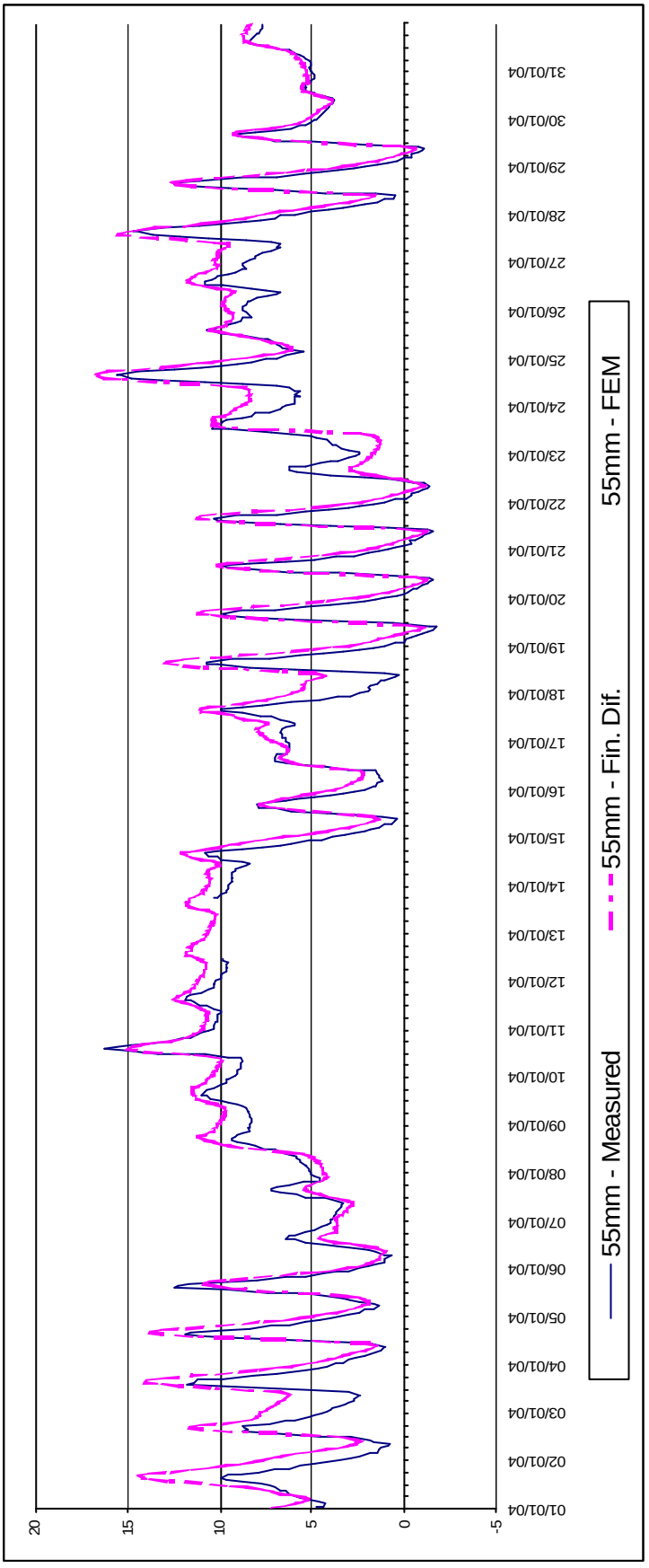

Figure 6 – January 55 mm-depth temperature distribution

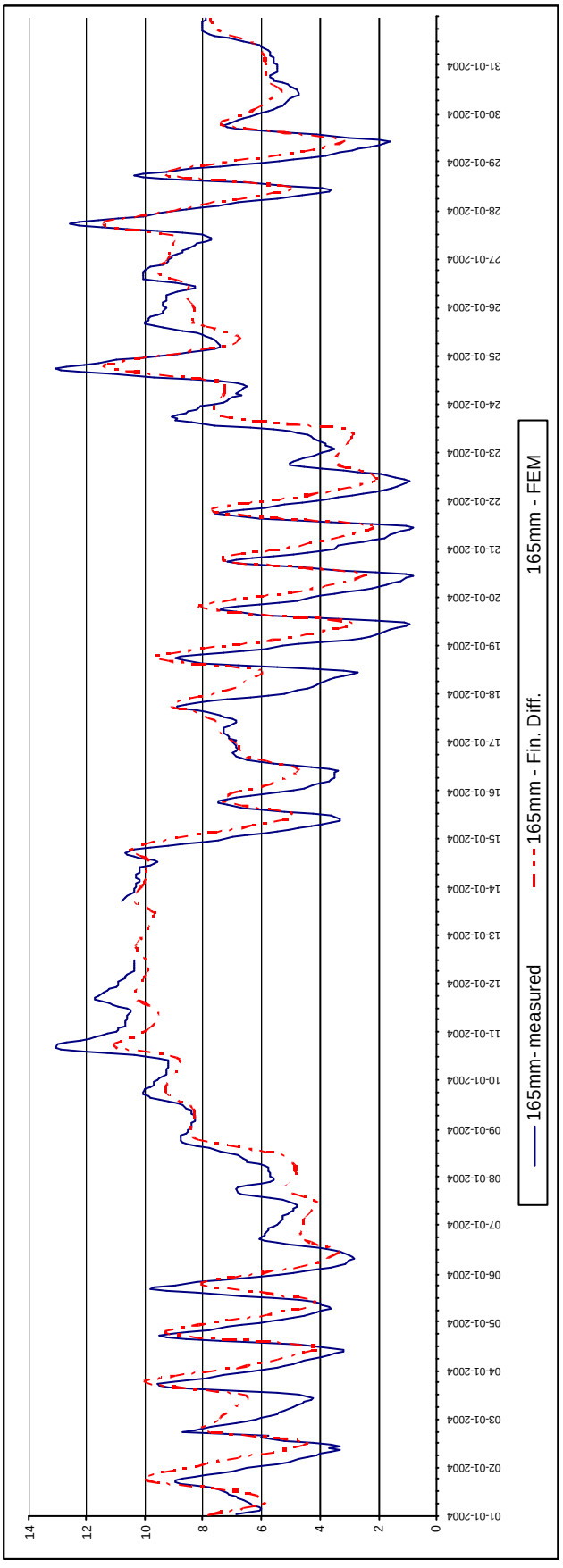

Figure 7 – January 165 mm –depth Temperature distribution

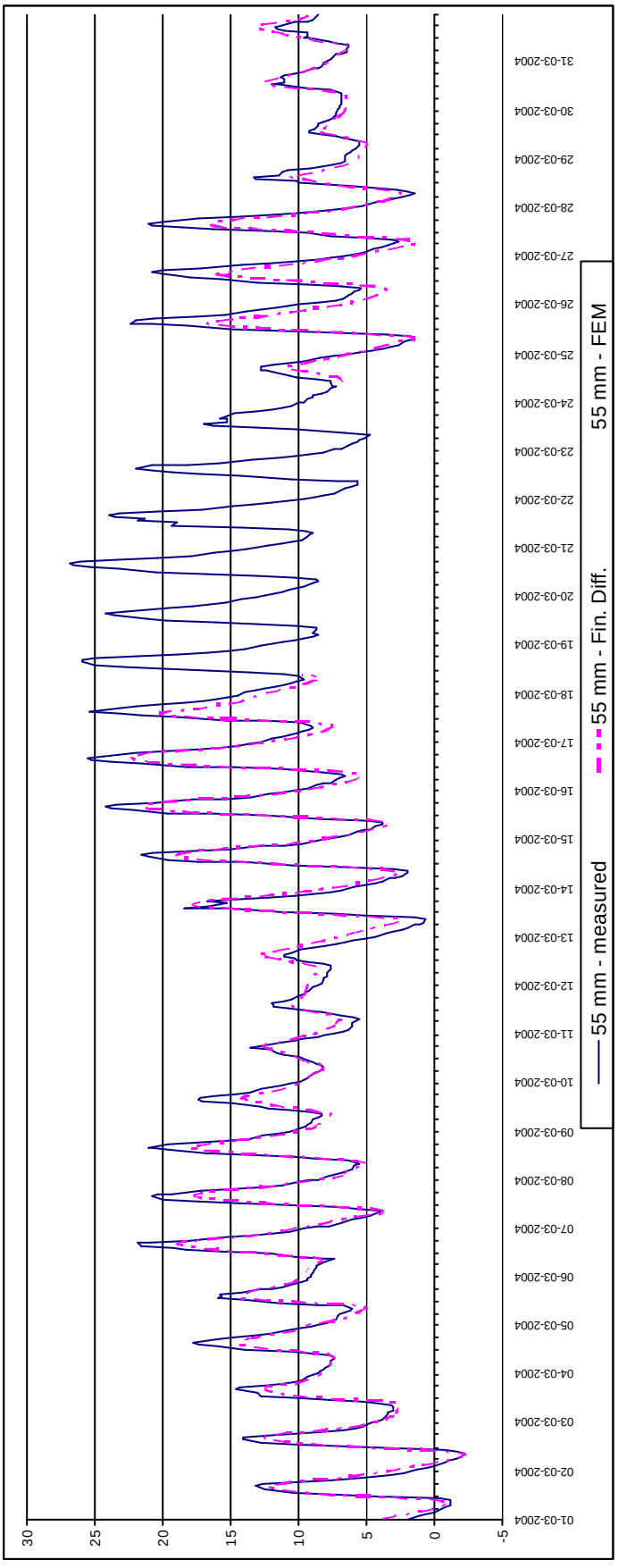

Figure 8 – March 55 mm –depth Temperature distribution

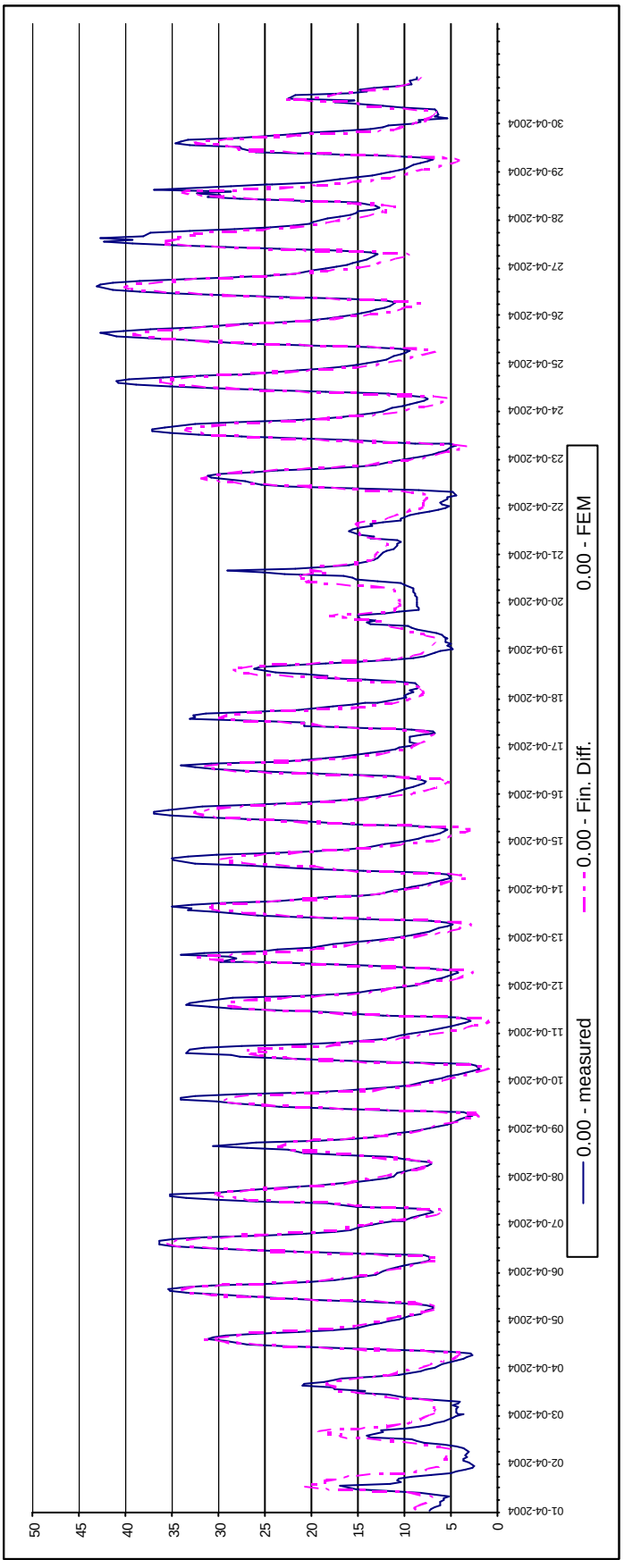

Figure 8 – April 0.0 mm-depth temperature distribution

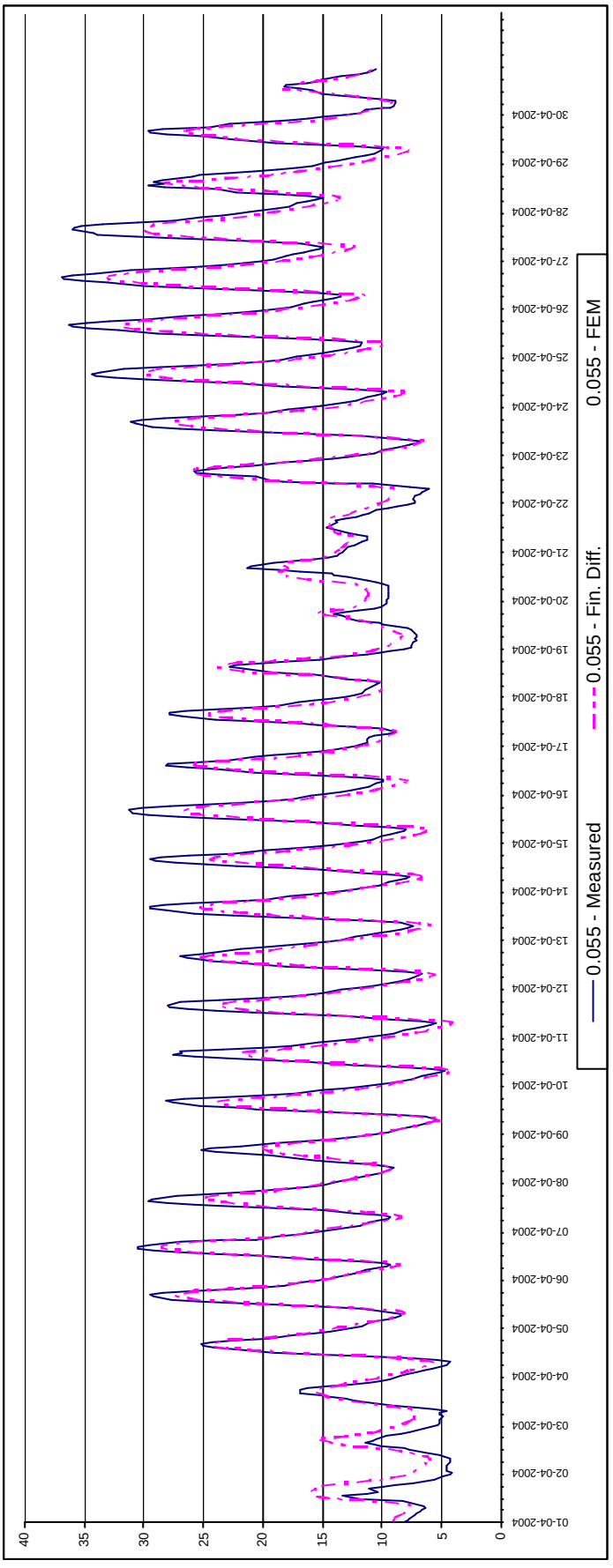

Figure 9 – April, 55mm-depth temperature distribution

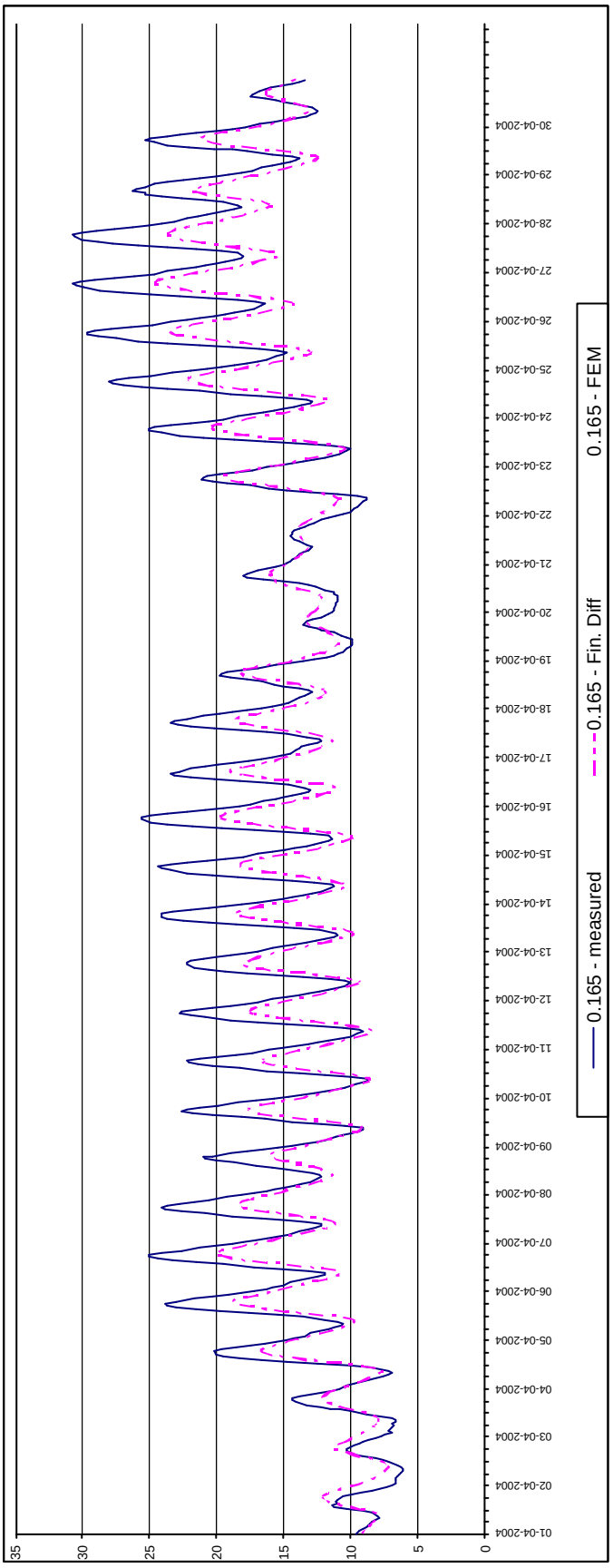

Figure 10 – April, 165mm-depth temperature distribution